Modern Mechanical Engineering, 2025, 15(2), 19-34
https://www.scirp.org/journal/mme
ISSN Online: 2164-0181
ISSN Print: 2164-0165

A Multidimensional Sequence Similarity-Based Approach for Engine Remaining Useful Life Prediction

Jie Lan[1,2], Zhining Li[1*], Jingnan Liu[2], Wenbin Luo[2]

[1]Shijiazhuang Campus of Army Engineering University, Shijiazhuang, China
[2]Units of the Chinese People's Liberation Army
Email: lanjie123456qwe@126.com, *13648990287@163.com

How to cite this paper: Lan, J., Li, Z.N., Liu, J.N. and Luo, W.B. (2025) A Multidimensional Sequence Similarity-Based Approach for Engine Remaining Useful Life Prediction. *Modern Mechanical Engineering*, **15**, 19-34.
https://doi.org/10.4236/mme.2025.152002

Received: April 23, 2025
Accepted: May 27, 2025
Published: May 30, 2025

Abstract

Similarity-based prediction modeling is a common method for estimating the remaining useful life (RUL) of a machine. The present study proposes a novel similarity-based multidimensional sequential approach to enhance the prediction accuracy of engine remaining useful life. The proposed approach involves the following steps: Initially, a screening of degradation-sensitive sensor variables is conducted through trend intensity analysis of all sensor data. Subsequently, historical degradation trajectories are constructed through polynomial fitting on selected sensor sequences. Then, multidimensional simultaneous sliding similarity matching is implemented between test samples and historical trajectories, with Manhattan distance summation serving as the similarity metric. Finally, the most similar historical trajectory segments are selected, and RUL reference values are derived from the most similar historical trajectories. Weighted RUL estimates are then calculated based on similarity levels. The validation using the C-MAPSS dataset demonstrates the efficacy of the method, with a root mean square error (RMSE) of 15.14 and a score function value of 334.18, thereby surpassing other methods in terms of computational simplicity and prediction accuracy.

Keywords

Aircraft Engine, Manhattan Distance, Prediction of Remaining Useful Life, Similarity Match

1. Introduction

The aerospace industry recognizes aircraft engines as the primary power source of modern aviation. These engines represent highly intricate and meticulously engineered systems, characterized by their advanced integration and sophisticated design. Their demanding operational environments impose exceptionally stringent requirements for safety and reliability. In this context, China's "14th Five-Year Plan for Civil Aviation Development" explicitly prioritizes the implementation of comprehensive life-cycle safety management systems for domestically manufactured civil aircraft. The strategic objective aims to maintain major accident rates in civil aviation operations below 0.11 incidents per million flight hours. Statistical analyses reveal that engine-related failures account for 50% of all civil aviation aircraft malfunctions, with corresponding maintenance costs exceeding 60% of total aircraft maintenance expenditures. These findings substantiate the critical need for adopting full-lifecycle condition management systems for aviation engines. This operational imperative underscores the necessity to develop robust Prognostics and Health Management (PHM) methodologies. Effective implementation of such systems promises to optimize aircraft maintenance costs while ensuring the highest standards of passenger safety and asset protection throughout operational service.

In Prognostics and Health Management (PHM), the term "prognosis" specifically denotes the prediction of Remaining Useful Life (RUL), defined as the operational time interval during which in-service equipment can maintain specified functionality under current operating conditions. Contemporary life prediction methodologies primarily fall into three categories: physical model-based approaches, data-driven techniques, and hybrid model-based solutions [1]-[3]. Among these, data-driven approaches have gained predominant adoption due to their ability to bypass the need for studying mechanical degradation mechanisms, instead leveraging historical operational data to construct RUL prediction models. These methods demonstrate relatively high prediction accuracy when sufficient historical samples are available. Data-driven RUL prediction techniques can be further classified into three principal types: similarity-based models [4]-[7], deep learning approaches [8]-[12], and statistical methods [13]-[19]. Similarity-based residual prediction methodologies operate by comparing test samples with historical degradation patterns, utilizing the RUL values of historical samples exhibiting maximum similarity as estimates for test specimens. Recent advancements in this field include: Liu developed a similarity health indicator combined with a Conditional Generative Adversarial Network (CGAN) prediction model, demonstrating effective early failure detection and precise characterization of rolling bearing performance degradation [20]. Liang proposed an enhanced similarity metric with degradation-sensitive weight allocation, enabling weighted RUL predictions through subsequent similarity matching [21]. Li introduced a Bayesian integrated RUL prediction method that clusters variable-length historical Run-to-Failure trajectories into distinct degradation patterns, employing pattern-specific kernel functions and similar trajectory libraries to construct Relevance Vector Machine (RVM) models with improved prediction accuracy [22]. Yu enhanced RUL prediction precision through effective variable selection using a lasso regression algorithm integrated with similarity-based life prediction formulae [23].

This study presents a RUL prediction framework for turbofan engines that leverages multidimensional operational sequence similarity. The proposed methodology incorporates two sequential processes: 1) implementation of a cubic polynomial-based denoising framework applied to historical engine operational data, followed by 2) similarity evaluation between the denoised historical sequences and target test units. Specifically, cubic polynomial regression is employed to attenuate high-frequency noise components in multidimensional sensor readings while maintaining essential degradation patterns. The processed sequences are then aligned with test samples through temporal sequence matching, enabling similarity-based RUL estimation through comparative analysis of multidimensional trajectory characteristics. Unlike conventional approaches [23]-[25] that first apply principal component analysis (PCA) and multiple linear regression for dimensionality reduction to establish one-dimensional health indicators prior to similarity analysis, our method preserves the nonlinear characteristics inherent in aero-engine degradation processes. Previous linear dimensionality reduction techniques risk losing critical nonlinear information that could compromise prediction accuracy. In contrast to data dimension reduction, our framework implements a multidimensional simultaneous moving similarity comparison between test data and noise-reduced historical degradation trajectories. The proposed similarity metric combines the summed Manhattan distances across multidimensional sequences, enabling comprehensive pattern matching. The RUL estimation derives from selecting multiple historical trajectory segments demonstrating highest similarity to test samples, with their corresponding RUL values serving as the reference basis for prognostic evaluation.

2. Theory and Method

2.1. Degradation-Sensitive Sensor Selection

Due to variations in data collection methodologies, sensor data types, installation locations, and other operational factors, significant discrepancies exist in how effectively different data types characterize engine faults. Consequently, identifying sensor data with strong correlations to engine degradation becomes critical for accurate RUL prediction based on degradation trend analysis. To address this, our study introduces a time-series trend indicator to systematically compare the degradation-related trend strength across sensor datasets. This indicator is defined by the following computational formula:

$$V_{trend} = \frac{\left|\sum_{i=1}^{N}\left(y_i-\overline{y}\right)\left(t_i-\overline{t}\right)\right|}{\sqrt{\sum_{i=1}^{N}\left(y_i-\overline{y}\right)^2\sum_{i=1}^{N}\left(t_i-\overline{t}\right)^2}} \tag{1}$$

where $\overline{y}$ is the mean value of the time series y_i, $\overline{t}$ is the mean value of the time vector t_i, N is the length of the series. The evaluation index is confined to the range $[0,1]$, with values closer to 1 indicating stronger trend manifestation in the sequence. After calculating the trendiness scores for all sensor data, we ranked them in descending order and subsequently selected those with higher rankings as valid inputs for RUL prediction.

2.2. Similarity Matching for Multidimensional Sequences

Sliding similarity matching involves sliding the test sample sequence incrementally along the historical degradation trajectory. At each step, the similarity between the test sequence and the corresponding segment of the historical trajectory is calculated. By traversing all possible positions on the historical trajectory, the method systematically identifies the segment that exhibits the highest similarity to the test sequence. This process, illustrated in Figure 1, enables precise alignment of the test sequence with the most relevant segment of the historical degradation pattern.

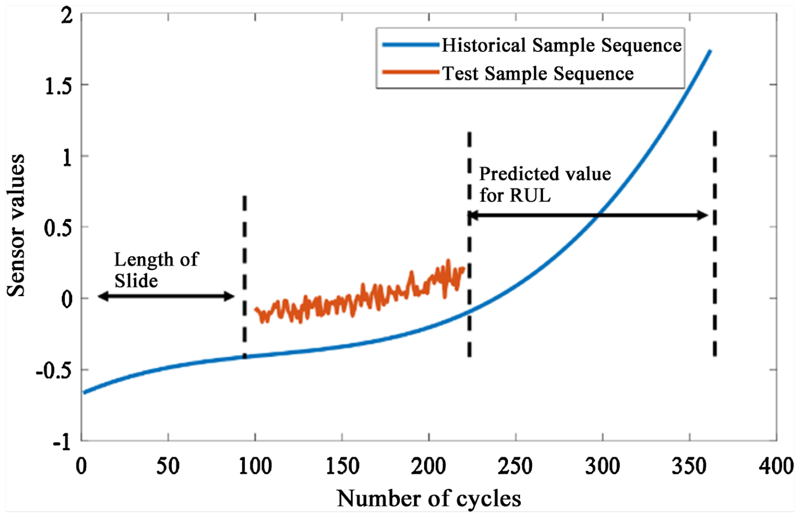

Figure 1. Sliding similarity matching process.

The raw sensor data contains significant noise, and directly applying similarity matching to such data may result in elevated matching errors due to noise interference. To address this issue, this paper employs a third-degree polynomial to denoise the raw sensor sequence. The fitted curve generated through this process is adopted as the degradation trajectory. The mathematical representation of the polynomial fitting is as follows:

$$y = at^3 + bt^2 + ct + d \tag{2}$$

where t is the time vector corresponding to the time series, y is the fitted data series, (a, b, c, d) are polynomial coefficients.

The multi-dimensional degradation data from historical engine samples are processed using the predefined noise reduction model. For example, with 100 historical engine degradation samples (each containing 21 multi-dimensional sensor sequences), a total of 100 × 21 smoothed degradation trajectory curves are generated by this fitting method.

While Euclidean distance is commonly employed to quantify similarity between sequences, studies in the literature [26] demonstrate that Manhattan distance-based similarity matching outperforms Euclidean distance for remaining useful life (RUL) prediction. Consequently, this paper adopts Manhattan distance to measure the similarity between test sample sequences and historical degradation trajectories. The distance is calculated using the following formula:

$$D=\sum_{i=1}^{N}\left|z_i-y_i\right| \tag{3}$$

To avoid information loss caused by data dimensionality reduction or fusion, this paper proposes a multidimensional sequence synchronization-based similarity matching method. The similarity between multidimensional sequences is quantified using the Manhattan distance, with the calculation defined as follows:

$$D(S)=\min\sum_{l=1}^{m}\sum_{i=1}^{N}\left|z_{(l,i)}-y'_{(l,i+S)}\right| \tag{4}$$

where N is the length of the sequence, m is the dimension of the sequence, z is the test sample multidimensional sequence, y is the historical sample multidimensional sequence, S is the distance that the test sample slides over the historical sample. By systematically evaluating all positions along the historical degradation trajectory, the test sample sequence identifies the segment with the highest similarity. Once the optimal matching position is determined, the RUL reference value for the test sample is estimated using the prescribed formula:

$$RUL=M-\left(N+S_{match}\right)+1 \tag{5}$$

where RUL is the remaining life of the test specimens, M is the total length of the historical specimens, N is the length of the test specimens, S_{match} is the length of the test samples sliding relative to the training set samples when the similarity is highest. Using the above formula, the similarity of all historical samples to the test sample is calculated and sorted in descending order, and the first n similarity values are selected to form the set $\boldsymbol{D}=\left\{D_1,D_1,D_3,\cdots,D_n\right\}$, and their corresponding RUL reference values form the set $\boldsymbol{R}=\left\{RUL_1,RUL_2,\cdots,RUL_n\right\}$. **Figure 2** illustrates the RUL prediction methodology.

2.3. Calculating RUL

After computing sets $\boldsymbol{D}$ (distances) and $\boldsymbol{R}$, each RUL in set R is assigned a weight proportional to its corresponding similarity score. The final RUL estimate for the test sample is derived as the weighted average of these reference values, calculated using the following formula:

$$w_i=\frac{\frac{1}{D_i}}{\sum_{i=1}^{q}\frac{1}{D_i}} \tag{6}$$

$$Rul=\sum_{i=1}^{n}w_i\cdot Rul_i \tag{7}$$

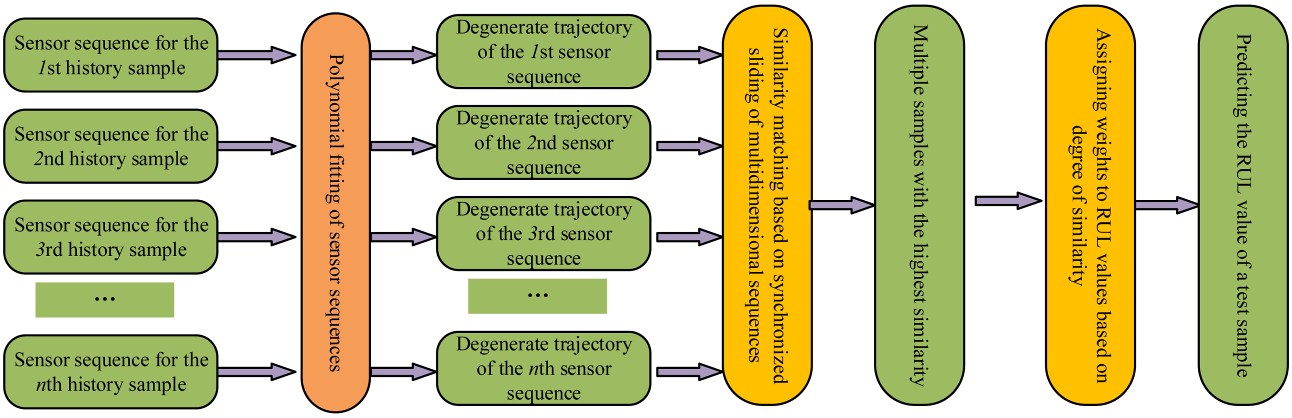

Figure 2. Flow of RUL prediction method based on multidimensional sequence similarity.

3. Experimentation

3.1. Experimental Data

The C-MAPSS aero-engine simulation dataset is widely adopted for validating RUL prediction methodologies. This dataset contains three operational state parameters and 21 sensor measurements recorded across each operational cycle of an aero-engine's lifecycle, spanning from initial healthy operation to eventual failure [27]. The specific sensor types and their descriptions are provided in **Table 1**. In this study, the FD001 subset of the C-MAPSS dataset is selected to evaluate the effectiveness of the proposed RUL prediction framework. The FD001 subset comprises 100 complete run-to-failure degradation trajectories and 100 partial degradation sequences for which RUL predictions are required.

Table 1. 21 sensor types in the C-MAPSS dataset.

Symbol	Description	Units
T2	Total temperature at fan inlet	˚R
T24	Total temperature at LPC outlet	˚R
T30	Total temperature at HPC outlet	˚R
T50	Total temperature at LPT outlet	˚R
P2	Pressure at fan inlet	Psia
P15	Total pressure in bypass-duct	psia
P30	Total pressure at HPC outlet	psia
Nf	Physical fan speed	rpm
Nc	Physical core speed	rpm
epr	Engine pressure ratio (P50/P2)	—
Ps30	Static pressure at HPC outlet	psia
phi	Ratio of fuel flow to Ps30	pps/psi
NRf	Corrected fan speed	rpm

Continued

NRc	Corrected core speed	rpm
BPR	Bypass Ratio	—
farB	Burner fuel-air ratio	—
htBleed	Bleed Enthalpy	—
Nf_dmd	Demanded fan speed	rpm
PCNfR_dmd	Demanded corrected fan speed	rpm
W31	HPT coolant bleed	lbm/s
W32	LPT coolant bleed	lbm/s

Due to the unique characteristics of the C-MAPSS dataset, the cycle length of each engine under different operating conditions varies—whether in the training set or the test set. In the FD001 subset, the minimum lifespan is 31 cycles. To maximize information retention when matching test samples with training samples for similarity, this study uniformly sets the sliding window width to 30 and the sliding step to 1. Each slide operation triggers one similarity matching process.

3.2. Data Preprocessing

The 21 variables in the dataset exhibit varying scales and therefore require normalization prior to analysis. The normalization is performed using the following formula:

$$norm\left(y_{(n,m)}\right)=\frac{y_{(n,m)}-mean\left(y_m\right)}{std\left(y_m\right)} \tag{8}$$

where $mean(y_m)$ and $std(y_m)$ are the mean and standard deviation of the values of the mth variable in all samples of the training set, $y(n,m)$ is the data sequence of the mth variable in the nth sample, $norm(y_{n,m})$ is the sequence of values after normalization of the sequence.

After normalization, the degradation trend indicators for the 21 sensor variables were computed using Formula (1). The indicator results were derived by averaging the trend indicator values across all 100 historical samples. These 21 sensor-based trend indicators were then ranked in descending order of significance, as summarized in **Table 2**. The analysis reveals that Sensors #11, #12, #4, #7, #15, #21, #20, #13, #8, #14, #2, #17, #3, and #9 exhibit the most pronounced degradation-related trends during the engine's operational lifespan. This finding validates their relevance and suitability as critical inputs for RUL prediction. The data trends recorded by the remaining sensors (positions 1, 5, 6, 10, 16, and 18) indicate values of 0, demonstrating that there is no statistically significant correlation between the measured parameters (including six types of parameters such as fan inlet total temperature, fan inlet pressure, and bypass duct total pressure) and the engine performance degradation. Consequently, these datasets have been excluded from the effective predictive parameters for engine health monitoring. **Figure 3** further clearly

Table 2. Trend indicators for 21 types of sensors.

Serial No.	11	12	4	7
Trend Indicator	0.811	0.79	0.782	0.762
Serial No.	15	21	20	13
Trend Indicator	0.727	0.718	0.714	0.687
Serial No.	8	14	2	17
Trend Indicator	0.684	0.681	0.675	0.673
Serial No.	3	9	1	5
Trend Indicator	0.644	0.643	0	0
Serial No.	6	10	16	18
Trend Indicator	0	0	0	0
Serial No.	19			
Trend Indicator	0			

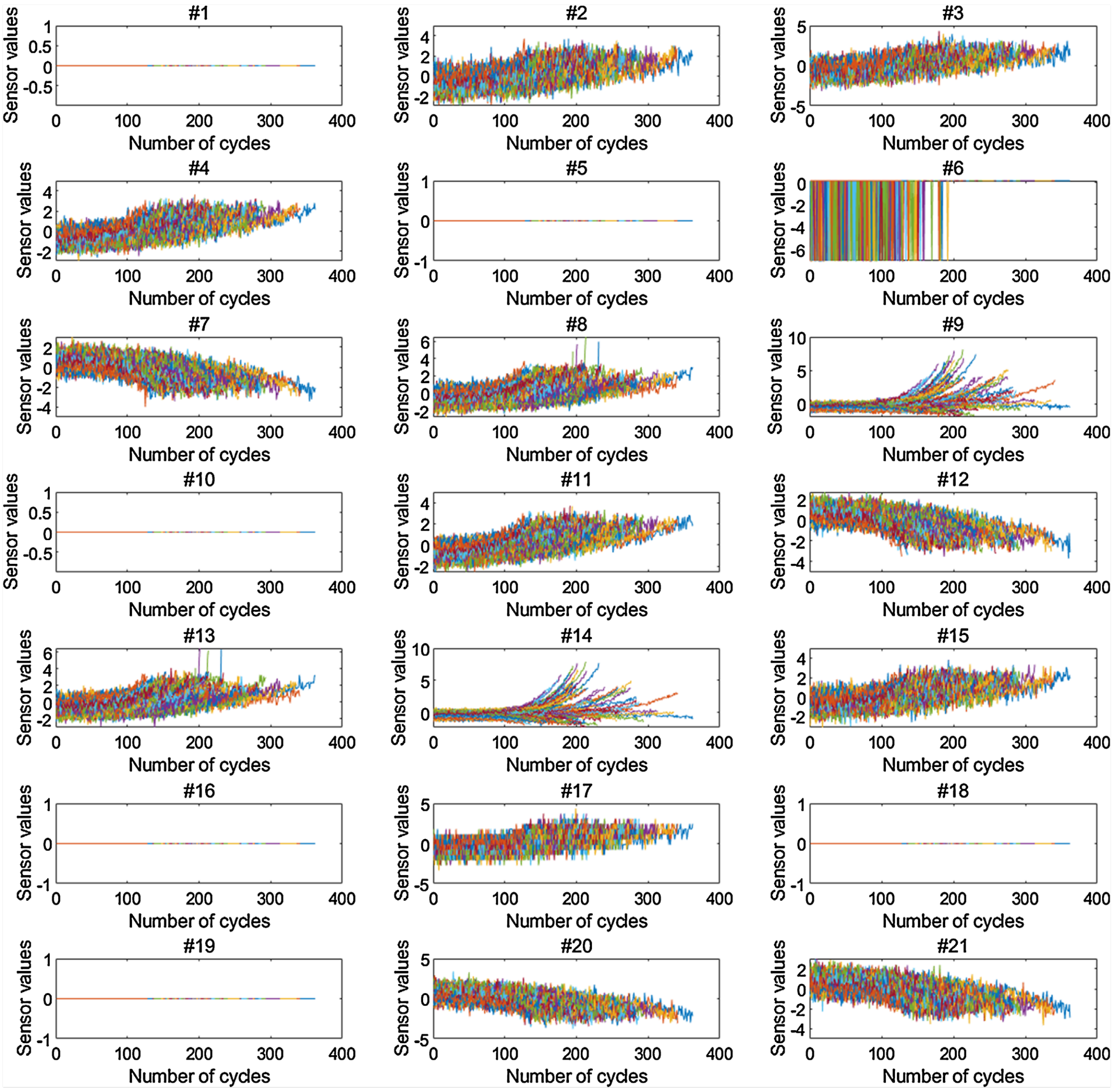

Figure 3. Numerical images of 21 types of sensors.

demonstrates that the above six parameters exhibit no discernible trend of change.

A third-degree polynomial fitting is applied to the 14-dimensional full-life degradation sequences of all 100 historical samples, generating 100 smoothed degradation trajectories. Figure 4 below compares the normalized raw sequences with the polynomial-fitted sequences for the high-pressure compressor outlet total temperature across all training set samples. As shown, the raw sensor data exhibits significant noise, whereas the fitted trajectories effectively capture the underlying degradation trend of the engine.

During the engine's healthy operational phase, wear is minimal, and the RUL is typically assumed to remain stable. Directly adopting the actual RUL value as the reference for test samples could lead to overestimated predictions. To mitigate this, historical RUL values are adjusted by capping the maximum RUL at 130 operational cycles. Figure 5 illustrates the adjusted RUL profile for the first engine

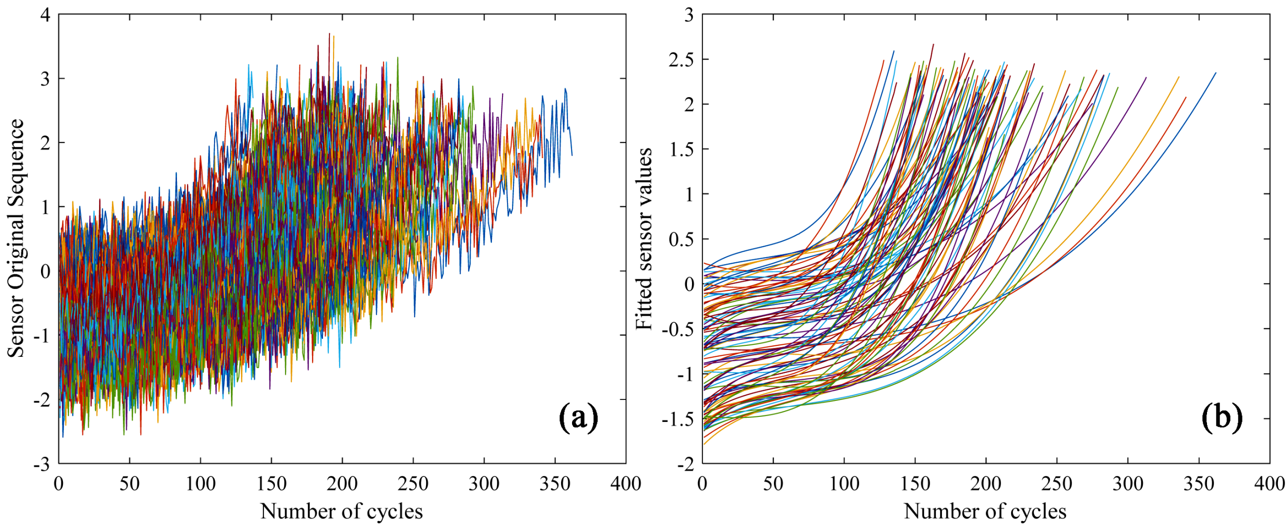

Figure 4. Original sequence (a) and fitted sequence after noise reduction (b) for the 7th sensor of 100 training set samples.

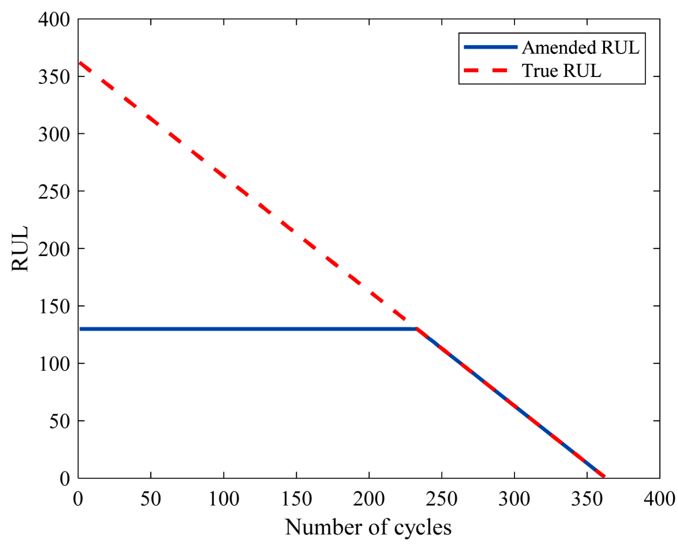

Figure 5. Schematic diagram of the correction of RUL.

in the training set, demonstrating this correction process.

3.3. Evaluation Function

To evaluate the accuracy of remaining useful life (RUL) predictions for aero-engines, two metrics are widely adopted: the root mean square error (RMSE) and a custom scoring function (Score). Lower values for both metrics indicate higher prediction accuracy. In engineering practice, overestimation of RUL (predicted values exceeding actual values) poses significantly greater operational risks than underestimation. To account for this, the scoring function imposes a disproportionately higher penalty on overestimations. The mathematical definitions of these evaluation metrics are as follows:

$$error_i = Rul_{predict} - Rul_{true} \tag{9}$$

$$RMSE = \sqrt{\frac{1}{n}\sum_{i=1}^{n} error_i^2} \tag{10}$$

$$Score = \begin{cases} \sum_{i=1}^{I} \exp\left(\frac{-error_i}{13}\right), & error_i < 0 \\ \sum_{i=1}^{I} \exp\left(\frac{error_i}{10}\right), & error_i > 0 \end{cases} \tag{11}$$

4. Experimental Results and Analysis

4.1. Experimental Results

The performance of the similarity-based remaining useful life (RUL) prediction method is influenced by the number of RUL reference values included in the analysis. Figure 6 demonstrates the relationship between the quantity of reference

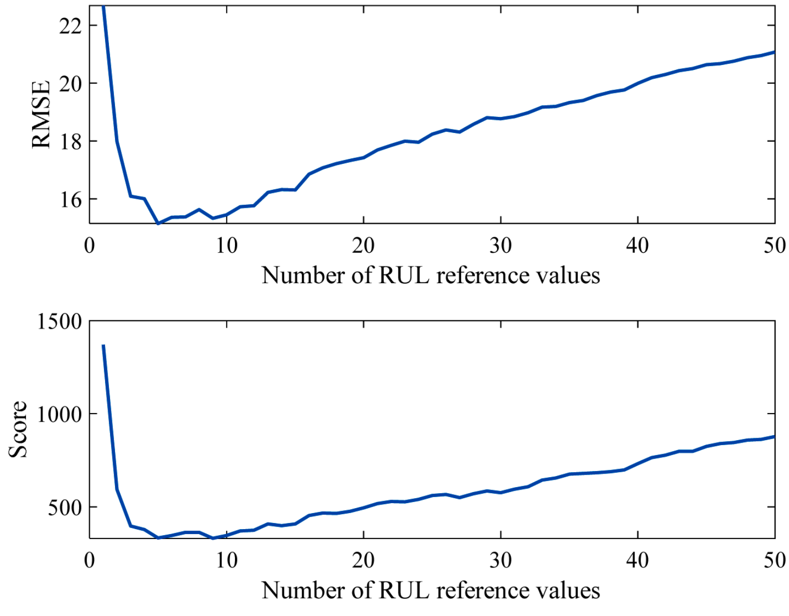

Figure 6. Effect of the number of RUL reference values on prediction accuracy.

values and prediction accuracy. As shown, both the root mean square error (RMSE) and the scoring function (Score) reach their minimum values when five reference values are selected, indicating optimal prediction performance. Under this configuration, the RMSE is 15.14, and the Score is 334.18. Figure 7 displays the RUL prediction results for the 100 test set samples using five reference values, with test samples sorted in descending order based on their actual RUL values.

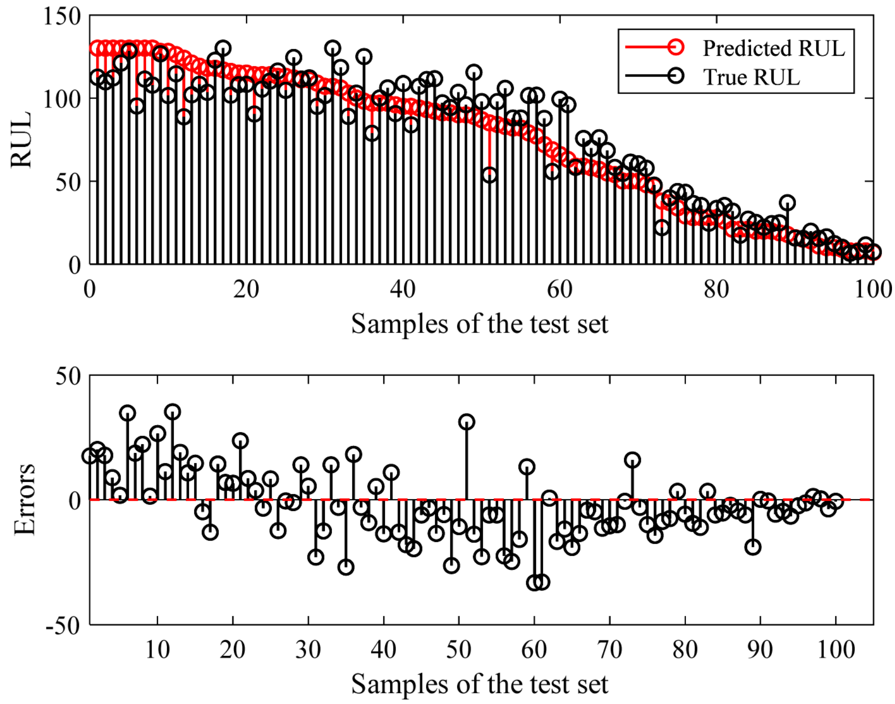

Figure 7. RUL prediction results for 100 test set samples.

To validate the effectiveness and generalizability of the proposed method, RUL predictions were performed for four test engines (#31, #56, #76, and #92) across the temporal dimension. The prediction results, illustrated in Figure 8, demonstrate the method's robust capability to accurately estimate RUL throughout the entire operational lifecycle of the engines.

4.2. Comparison of Results with Other Prediction Method

The choice of statistical indicators for fusing RUL reference values significantly influences prediction outcomes. This study evaluates three fusion strategies: using the mean, median, and maximum probability density values of the RUL reference values as estimates for test samples. As demonstrated in Table 3, the weighted fusion approach—which prioritizes reference values based on their similarity to test sequences—achieves the highest prediction accuracy compared to the other statistical methods.

To highlight the advantages of the proposed method, its performance was evaluated against state-of-the-art approaches from the literature [28]-[33]. As summarized in Table 4, the results demonstrate that the proposed method

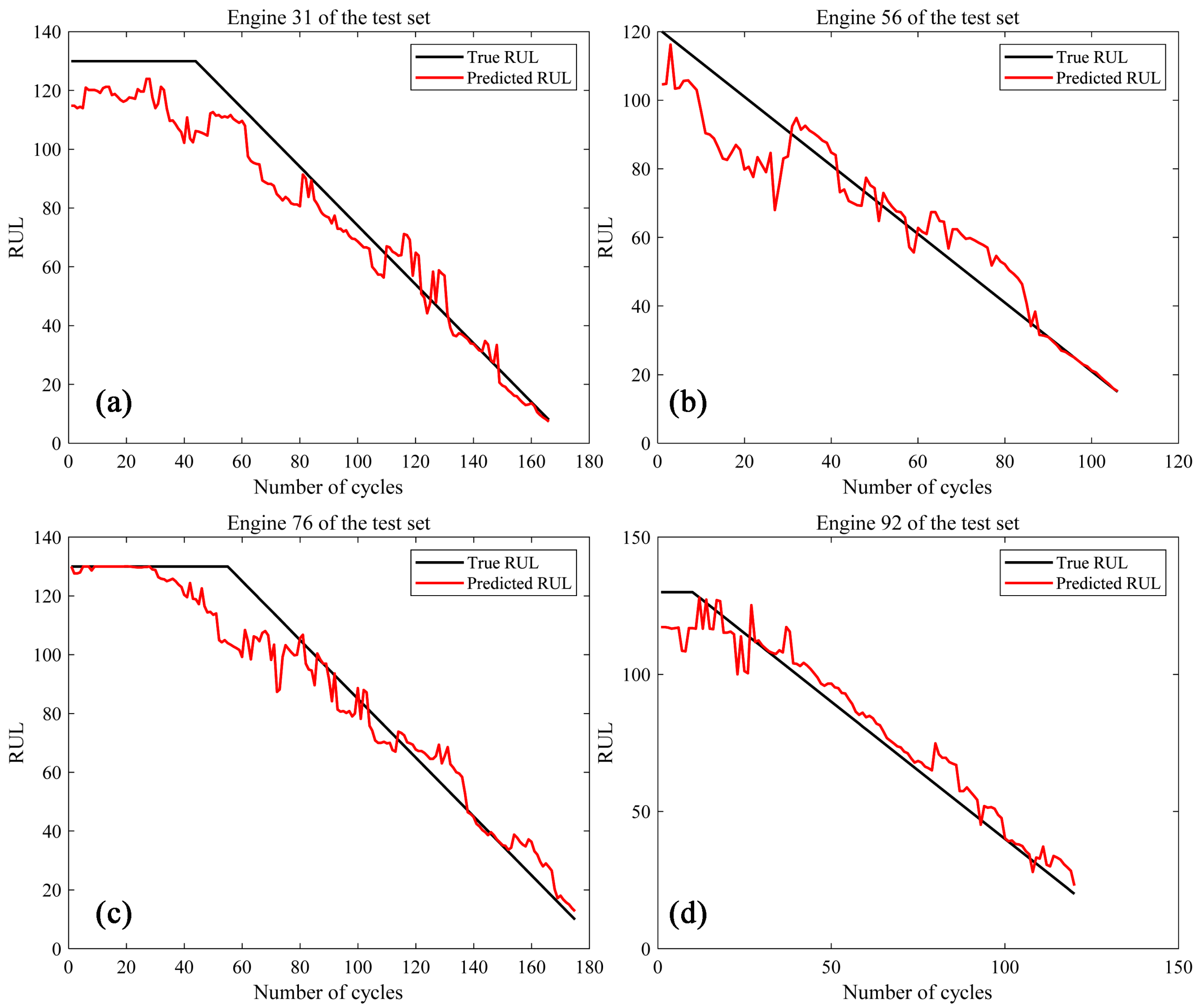

Figure 8. RUL predictions for the test set of four engines during operation.

Table 3. Comparison of results with different fusion methods.

Integration method	Optimal number of RUL reference values	RMSE	Score
Based on average values	5	15.24	346.2
Based on median	9	15.46	353.3
Based on the maximum probability density	9	15.56	378.8
Proposed method	5	15.14	334.18

Table 4. Comparison of results of different RUL prediction models for FD001 dataset.

Models	RMSE	Score
Random Forest [28]	17.88	517.54
SVM [29]	29.822	-
LSTM [30]	16.14	338

Continued

FM [31]	17.91	480
DLLSTM [32]	18.33	655
NSC [33]	16.7	-
Based on biexponential fitting	19.7	724
Based on a fourth-degree polynomial fit	15.06	450.84
Based on no noise reduction	21.1	2557
Proposed method	15.14	334.18

achieves superior prediction accuracy compared to all benchmarked methods. Additionally, we compared the proposed method with three alternative approaches: quartic polynomial fitting, double exponential fitting, and no fitting. The results demonstrate that both the double exponential fitting and no fitting methods yield significantly lower prediction accuracy than our proposed approach. While the quartic polynomial fitting method achieves comparable RMSE to our method, its Score metric is higher. However, this approach requires computing more parameters during the fitting process. These comparative results collectively validate the effectiveness and superiority of our proposed cubic polynomial fitting-based denoising method.

4.3. Analysis of Results

The results show that the RUL prediction method based on multi-dimensional sequence similarity proposed in this paper has higher prediction accuracy compared with the above-mentioned multi-class prediction models. Meanwhile, the proposed method does not require dimensionality reduction and fusion or feature extraction of multi-dimensional data, nor does it need extensive sample training and network parameter optimization like deep learning algorithms such as LSTM. Therefore, the proposed method in this paper has the advantages of simple modeling and high accuracy.

The results demonstrate that the proposed multidimensional sequence similarity-based RUL prediction method achieves superior accuracy relative to the aforementioned multivariable prediction models. Furthermore, unlike machine learning approaches such as LSTM—which require extensive sample training and hyperparameter optimization—the proposed method eliminates the need for dimensionality reduction, data fusion, or manual feature extraction of multidimensional sensor data. This dual advantage of simplified modeling and high precision positions the method as an efficient and practical solution for remaining useful life estimation in industrial applications.

5. Conclusion

This study proposes a remaining useful life prediction method based on multidimensional sequence similarity, validated using the NASA C-MAPSS aero-engine simulation dataset. The results demonstrate that the method achieves high accuracy across the 100 test samples and exhibits consistent performance throughout the engine's entire operational lifespan, confirming its validity and generalizability. Comparative analysis with existing approaches from the literature further highlights the method's advantages, including simplified implementation and superior precision relative to conventional techniques. However, the current framework relies on fixed-length sequence matching for similarity calculations, which occasionally leads to suboptimal predictions for individual edge cases. Addressing this limitation through adaptive sequence length optimization represents a key direction for future research.

Conflicts of Interest

The authors declare no conflicts of interest regarding the publication of this paper.

References

[1] Lu, S., Su, Y., Yang, M. and Li, Y. (2018) A Modified Walker Model Dealing with Mean Stress Effect in Fatigue Life Prediction for Aeroengine Disks. *Mathematical Problems in Engineering*, **2018**, 1-12. https://doi.org/10.1155/2018/5148278

[2] Li, F., Shang, D., Zhang, C., Liu, X., Li, D., Wang, J., *et al.* (2019) Thermomechanical Fatigue Life Prediction Method for Nickel-Based Superalloy in Aeroengine Turbine Discs under Multiaxial Loading. *International Journal of Damage Mechanics*, **28**, 1344-1366. https://doi.org/10.1177/1056789519831050

[3] Gouriveau, R., Medjaher, K. and Zerhouni, N. (2016) From Prognostics and Health Systems Management to Predictive Maintenance. Wiley. https://doi.org/10.1002/9781119371052

[4] Gu, M.Y., Dai, Z.X., Wu, H.T. and Xu, X.S. (2024) Similarity-Based Residual Life Prediction Method Based on Dynamic Time Scale and Local Similarity Search. *Journal of the Brazilian Society of Mechanical Sciences and Engineering*, **46**, Article No. 276. https://doi.org/10.1007/s40430-024-04857-3

[5] Gu, M.Y., Ge, J.Q. and Li, Z.N. (2023) Improved Similarity-Based Residual Life Prediction Method Based on Grey Markov Model. *Journal of the Brazilian Society of Mechanical Sciences and Engineering*, **45**, Article No. 294. https://doi.org/10.1007/s40430-023-04176-z

[6] Luo, H., Bo, L., Liu, X. and Zhang, H. (2021) A Novel Method for Remaining Useful Life Prediction of Roller Bearings Involving the Discrepancy and Similarity of Degradation Trajectories. *Computational Intelligence and Neuroscience*, **2021**, Article 2500997. https://doi.org/10.1155/2021/2500997

[7] Ma, B., Yan, S., Wang, X., Chen, J. and Zheng, C. (2020) Similarity-Based Failure Threshold Determination for System Residual Life Prediction. *Eksploatacja i Niezawodność—Maintenance and Reliability*, **22**, 520-529. https://doi.org/10.17531/ein.2020.3.15

[8] Sun, B., Hu, W., Wang, H., Wang, L. and Deng, C. (2025) Remaining Useful Life Prediction of Rolling Bearings Based on CBAM-CNN-LSTM. *Sensors*, **25**, Article 554. https://doi.org/10.3390/s25020554

[9] Shang, J., Xu, D., Li, M., Qiu, H., Jiang, C. and Gao, L. (2025) Remaining Useful Life Prediction of Rotating Equipment under Multiple Operating Conditions via Multi-

Source Adversarial Distillation Domain Adaptation. *Reliability Engineering & System Safety*, **256**, Article 110769. https://doi.org/10.1016/j.ress.2024.110769

[10] Wang, J., Lu, Z., Zhou, J., Schröder, K. and Liang, X. (2025) A Novel Remaining Useful Life Prediction Method under Multiple Operating Conditions Based on Attention Mechanism and Deep Learning. *Advanced Engineering Informatics*, **64**, Article 103083. https://doi.org/10.1016/j.aei.2024.103083

[11] Wang, C., Jiang, W., Shi, L. and Zhang, L. (2025) Rolling Bearing Remaining Useful Life Prediction Using Deep Learning Based on High-Quality Representation. *Scientific Reports*, **15**, Article No. 8228. https://doi.org/10.1038/s41598-025-93165-4

[12] Wang, L., Cao, H. and Chen, X. (2025) Information Guided Attention Network for Bearing Remaining Useful Life Prediction Adaptive to Working Conditions and Fault Modes. *Engineering Applications of Artificial Intelligence*, **147**, Article 110197. https://doi.org/10.1016/j.engappai.2025.110197

[13] Wu, X., Yang, X., Huang, J. and Peng, K. (2023) Remaining Useful Life Prediction for Motor Systems by Iteratively Updated Wiener Process Based on Closed-Loop Performance Degradation Monitoring. *Proceedings of the Institution of Mechanical Engineers, Part I: Journal of Systems and Control Engineering*, **238**, 3-15. https://doi.org/10.1177/09596518231199770

[14] Liu, Q., Liu, W., Dong, M., Li, Z. and Zheng, Y. (2023) Residual Useful Life Prognosis of Equipment Based on Modified Hidden Semi-Markov Model with a Co-Evolutional Optimization Method. *Computers & Industrial Engineering*, **182**, Article 109433. https://doi.org/10.1016/j.cie.2023.109433

[15] Li, Y., Huang, X., Gao, T., Zhao, C. and Li, S. (2023) A Wiener-Based Remaining Useful Life Prediction Method with Multiple Degradation Patterns. *Advanced Engineering Informatics*, **57**, Article 102066. https://doi.org/10.1016/j.aei.2023.102066

[16] Gu, M.Y., Ge, J.Q. and Li, Z.N. (2023) Improved Similarity-Based Residual Life Prediction Method Based on Grey Markov Model. *Journal of the Brazilian Society of Mechanical Sciences and Engineering*, **45**, Article No. 294. https://doi.org/10.1007/s40430-023-04176-z

[17] Zhang, S., Zhang, Y. and Zhu, D. (2015) Residual Life Prediction for Rolling Element Bearings Based on an Effective Degradation Indicator. *Journal of Failure Analysis and Prevention*, **15**, 722-729. https://doi.org/10.1007/s11668-015-0003-z

[18] Zhang, Z., Peng, C. and Che, Z. (2020) Bayesian Online Change Point Detection Method for Process Monitoring. *2020 Chinese Control and Decision Conference* (*CCDC*), Hefei, 22-24 August 2020, 3389-3393. https://doi.org/10.1109/CCDC49329.2020.9164236

[19] Ta, Y., Li, Y. and Cai, W. (2023) Adaptive Staged Remaining Useful Life Prediction Method Based on Multi-Sensor and multi-Feature Fusion. *Reliability Engineering & System Safety*, **231**: 109033. https://doi.org/10.1016/j.ress.2022.109033

[20] Yang, L., Binbin, D., Cancan, Y., Shuhang, L., Xuguo, Y. and Han, X. (2024) Similarity Indicator and CG-CGAN Prediction Model for Remaining Useful Life of Rolling Bearings. *Measurement Science and Technology*, **35**, Article 086107. https://doi.org/10.1088/1361-6501/ad41f7

[21] Zeming, L., Jianmin, G., Hongquan, J., Xu, G., Zhiyong, G. and Rongxi, W. (2018) A Similarity-Based Method for Remaining Useful Life Prediction Based on Operational Reliability. *Applied Intelligence*, **48**, 2983-2995. https://doi.org/10.1007/s10489-017-1128-4

[22] Li, Z., Zheng, H., Xiang, X., Liu, S. and Wan, Y. (2025) Remaining Useful Life Prediction with Limited Run-to-Failure Data: A Bayesian Ensemble Approach Combin-

ing Mode-Dependent RVM and Similarity. *ISA Transactions*, **156**, 307-319. https://doi.org/10.1016/j.isatra.2024.11.023

[23] Yu, Q., Li, J., Dai, H. and Xin, F. (2023) Lasso Based Variable Selection for Similarity Remaining Useful Life Prediction of Aero-Engine. *Journal of Aerospace Power*, **38**, 931-938. https://doi.org/10.13224/j.cnki.jasp.20210516

[24] Lv, D. and Hu, Y. (2021) Remaining Useful Life Prediction of Aeroengine Based on Principal Component Analysis and One Dimensional Convolutional Neural Network. *Transactions of Nanjing University of Aeronautics and Astronautics*, **38**, 867-875. https://doi.org/10.16356/j.1005-1120.2021.05.014

[25] Cao, H., Cui, K. and Liang, J. (2020) Multrparameter Fusion Similarity-Based Method for Remaining Useful Life Predicition of Civil Aviation Engines. *China Mechanical Engineering*, **31**, 781-787. https://doi.org/10.3969/j.issn.1004-132X.2020.07.003

[26] Zhang, J., Wang, P., Yan, R. and Gao, R.X. (2018) Long Short-Term Memory for Machine Remaining Life Prediction. *Journal of Manufacturing Systems*, **48**, 78-86. https://doi.org/10.1016/j.jmsy.2018.05.011

[27] Saxena, A., Goebel, K., Simon, D. and Eklund, N. (2008) Damage Propagation Modeling for Aircraft Engine Run-to-Failure Simulation. 2008 *International Conference on Prognostics and Health Management*, Denver, 6-9 October 2008, 1-9. https://doi.org/10.1109/phm.2008.4711414

[28] Wang, H., Li, D., Li, D., Liu, C., Yang, X. and Zhu, G. (2023) Remaining Useful Life Prediction of Aircraft Turbofan Engine Based on Random Forest Feature Selection and Multi-Layer Perceptron. *Applied Sciences*, **13**, Article 7186. https://doi.org/10.3390/app13127186

[29] Louen, C., Ding, S.X. and Kandler, C. (2013) A New Framework for Remaining Useful Life Estimation Using Support Vector Machine Classifier. 2013 *Conference on Control and Fault-Tolerant Systems* (*SysTol*), Nice, 9-11 October 2013, 228-233. https://doi.org/10.1109/systol.2013.6693833

[30] Zheng, S., Ristovski, K., Farahat, A. and Gupta, C. (2017) Long Short-Term Memory Network for Remaining Useful Life Estimation. 2017 *IEEE International Conference on Prognostics and Health Management* (*ICPHM*), Dallas, 19-21 June 2017, 88-95. https://doi.org/10.1109/icphm.2017.7998311

[31] Zhang, C., Lim, P., Qin, A.K. and Tan, K.C. (2017) Multi-Objective Deep Belief Networks Ensemble for Remaining Useful Life Estimation in Prognostics. *IEEE Transactions on Neural Networks and Learning Systems*, **28**, 2306-2318. https://doi.org/10.1109/tnnls.2016.2582798

[32] Wu, J., Hu, K., Cheng, Y., Zhu, H., Shao, X. and Wang, Y. (2020) Data-Driven Remaining Useful Life Prediction via Multiple Sensor Signals and Deep Long Short-Term Memory Neural Network. *ISA Transactions*, **97**, 241-250. https://doi.org/10.1016/j.isatra.2019.07.004

[33] Singh, S.K., Kumar, S. and Dwivedi, J.P. (2017) A Novel Soft Computing Method for Engine RUL Prediction. *Multimedia Tools and Applications*, **78**, 4065-4087. https://doi.org/10.1007/s11042-017-5204-x